This is a repository copy of *Machining distortion in asymmetrical residual stress profiles*.

White Rose Research Online URL for this paper:
http://eprints.whiterose.ac.uk/151965/

Version: Published Version

Article:
Bilkhu, R., Ayvar-Soberanis, S., Pinna, C. orcid.org/0000-0002-9079-1381 et al. (1 more author) (2019) Machining distortion in asymmetrical residual stress profiles. Procedia CIRP, 82. pp. 395-399. ISSN 2212-8271

https://doi.org/10.1016/j.procir.2019.04.346

Article available under the terms of the CC-BY-NC-ND licence (https://creativecommons.org/licenses/by-nc-nd/4.0/).

Reuse
This article is distributed under the terms of the Creative Commons Attribution-NonCommercial-NoDerivs (CC BY-NC-ND) licence. This licence only allows you to download this work and share it with others as long as you credit the authors, but you can't change the article in any way or use it commercially. More information and the full terms of the licence here: https://creativecommons.org/licenses/

Takedown
If you consider content in White Rose Research Online to be in breach of UK law, please notify us by emailing eprints@whiterose.ac.uk including the URL of the record and the reason for the withdrawal request.

eprints@whiterose.ac.uk
https://eprints.whiterose.ac.uk/

Available online at www.sciencedirect.com

ScienceDirect

Procedia CIRP 00 (2019) 000–000

www.elsevier.com/locate/procedia

17th CIRP Conference on Modelling of Machining Operations

Machining Distortion in Asymmetrical Residual Stress Profiles

Ravi Bilkhu[a], Sabino Ayvar-Soberanis[a], Christophe Pinna[b] , Tom McLeay[a]

[a]The University of Sheffield Advanced Manufacturing Research Centre, Park Wallis Way, Catcliffe, Rotherham,UK
[b]The University of Sheffield, Department of Mechanical Engineering, 3 Solly Street, Sheffield S1 4DE, UK

* * Corresponding author. Tel.: +44 (0) 114 222 7685. E-mail address: r.bilkhu@amrc.co.uk

Abstract

This paper presents the results from a set of experimental and computational studies of the effect of asymmetrical residual stress on machining distortion of Al-7050 alloy. Aluminum coupons were physically bolted together for heat treatment to generate the asymmetrical residual stress profiles; which were measured using neutron diffraction method in the bulk of the samples after the heat treatment stage, and after the first machining stage to investigate the residual stress redistribution. A machining distortion model was successfully implemented to investigate comprehensibly the impact of the layer material removal in terms of depths of cut on the redistribution of the residual stress profile into the part, and how this redistribution influences the distortions in the coupon. This investigation allowed determining a robust machining approach capable of predicting the final desired distortion tolerance after clamping, irrespective of the highly asymmetric residual stress condition of the coupon. On machine inspection and CMM measurements were also done to validate the outcomes of the machining distortion model.

© 2019 The Authors. Published by Elsevier B.V.
Peer-review under responsibility of the scientific committee of The 17th CIRP Conference on Modelling of Machining Operations, in the person of the Conference Chair Dr Erdem Ozturk and Co-chairs Dr Tom Mcleay and Dr Rachid Msaoubi.

Keywords: Asymmetrical Residual Stress; Finite Element; Al-7050 alloy; neutron diffraction; machining distortion, high speed machining, layer material removal

1. Introduction

In order to meet industrial demands of high productivity and to reduce lead times, many aluminium aerospace structural components need to be manufactured faster and with very high precision [1]. Regardless of the advantages of high speed machining of aluminium alloys, part distortion in manufacturing is an issue [1]. Distortion, one of the outcomes of the residual stress imbalance profile within the component, is the main cause of scrap in a manufacturing environment especially within the machining sector due to components exceeding the tolerances imposed in high performance components.

Machining distortion for aluminium alloys is highly influenced by the residual stresses carried forward from the heat treatment process, more so than other aerospace alloys (titanium, nickel, stainless steels [2]), and is not due to machining induced stresses for structures with thicknesses over 3 mm. For aluminium thin-walled components (less than 3mm thickness), the machining process induces stresses by plastic deformation affecting distortion [3].

In order to avoid distortion related problems, manufacturing companies sometimes increase the number of operations on a “trial and error” basis, change the work holding strategy, or “shot peen” the part to correct for distortion, all of which increase production costs and time [4]. It should be noted that although some of these techniques relieve the stresses, they are still sufficient enough to cause large distortions especially for thin monolithic structures.

It was not until the exploitation of numerical analysis in the early 1990’s that the first machining distortion models were created to help generate a better understanding of distortion in greater detail [5]. Following on from this a substantial amount of work was done in this area to understand, control and optimize distortion in manufacturing [6][7][8].

2212-8271 © 2019 The Authors. Published by Elsevier B.V.
Peer-review under responsibility of the scientific committee of The 17th CIRP Conference on Modelling of Machining Operations, in the person of the Conference Chair Dr Erdem Ozturk and Co-chairs Dr Tom Mcleay and Dr Rachid Msaoubi.

Previous research has not discussed the machining distortions in the presence of highly asymmetrical residual stress carried forward from the heat treatment process. The present work is focused on the selection and implementation of a finite element (FE) model as the tool to predict the desired distortion regardless of the highly asymmetrical residual stress condition of the part.

2. Experimental study

In order to generate the residual stress profiles and carry out the subsequent distortion analysis, two 250 x 100 x 50 mm rectangular coupons were prepared from an Aluminium alloy 7050 billet. Counterbore holes were created in order physically bolted together the coupon for heat treatment. Two ridges were created on the middle of the side faces of each coupon with dimensions of 5 x 10 mm. The ridges were created to have a reference measurement location where distortion measurements would be monitored throughout the machining trials.

2.1. Heat treatment for asymmetrical residual stress profiles

For the generation of the asymmetric bulk residual stress profiles, the pair of coupons were heated to 477 °C in a furnace as shown in Figure 1; and then quenched in normal tap water at 20 °C (+/- 3 °C). The blocks were quenched following the Heat Treatment Standard for Aerospace alloys AMS 2770 [9].The selected dimensions of the samples were based on a number of limiting factors; the furnace size, the quench tank size, and the mass of the specimens as they needed to be manipulated by hand. The temperature on the surface of the samples was monitored by a thermocouple. The operators sample handling technique during the quenching procedure was monitored extensively.

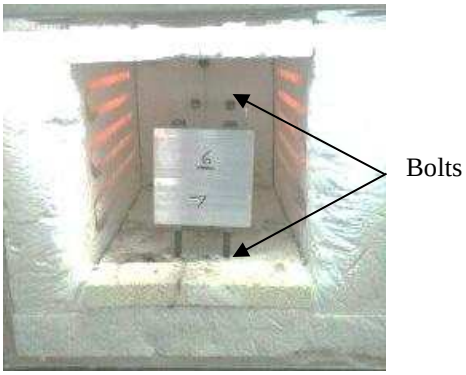

Fig. 1. Heat treatment strategy to generate asymmetric residual stress profiles

Neutron diffraction (ND) measurements were carried out by the Australian Nuclear Science and Technology Organisation (ANSTO) in order to capture the asymmetrical residual stress profiles in the blocks. The experimental residual stresses after quenching and the redistributed residual stresses after the machining of top face are compared with FE predictions in Section 4.

2.2. Machining tests

A Cincinnati FTV 5 machine was used for the experimental face milling machining trials. All coupons were constrained using finger clamps holding the sample at 25 mm from each end leaving a space of 200 mm for machining as shown in Figure 2. The objective of the machining trial was to finish off the coupons with a thickness of 20 mm regardless of the position of the machined section, and a distortion tolerance after clamping of 50 µm was set. The machining parameters are provided in Table 1. The axial depth of cut of the fist cut was 2 mm on both coupons. This increased to 3 mm. For cuts number 10, a 1 mm axial depth of cut was taken, followed by a final 3 mm depth of cut.

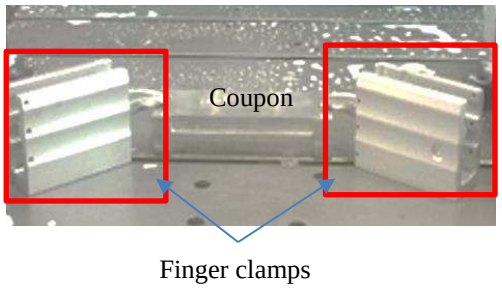

Fig. 2. Experimental set up for machining distortion analysis

Table 1. Machining parameters

Tool holder	25 mm diameter Sandvik R790
Insert	Grade H13A x 3
Cutting speed (v_c)	730 m/min
Feed rate (f_z)	0.2 m/min
Axial depth of cut (a_p)	0.4 - 3 mm
Radial depth of cut (a_e)	25 mm

To measure the distortion on the machine after each cut, a Renishaw MP700 probe was used. The probe had a 100 mm styli and 6 mm diameter ruby tip with a repeatability of 0.35 µm [10]. Additionally, a coordinate measuring machine (CMM) was used for post machining distortion measurements using a Leitz LSP-X1H probe with a 20 mm styli and a 3mm diameter.

3. Finite element model

DEFORM 2D/3D v11 (Scientific Forming Technology Co-operation) was used for stress and machining distortion simulations in this research. DEFORM simulations have previously been found to be useful in the prediction of machining distortion and residual stresses [11] and to have greater flexibility when compared to other finite element (FE) methods. This package uses a Lagrangian implicit code for its numerical calculations to predict the machining deformation and has been found to be capable in previous research work for the prediction of machining distortion [11][12].

3.1. Heat treatment model set up

The heating up of the coupons was simulated from room temperature to solution temperature (477 °C) over a period of 5 hours.

The heat treatment model was created using an elastic-plastic, Newton-Raphson iteration, and Langrangian incremental method. For the simulation to generate an asymmetric stress profile, an inter-object relationship was set up for the two workpieces joined together as shown in Figure 3 (a)); and the heat transfer coefficient (HTC) (Figure 3 (b)) was applied on the external faces of both parts except where the two samples are in contact with each other.

The HTC used was generated by recording the temperature within the coupon on the surface, the middle thickness and the bottom surface using thermocouples and converting this to the heat transfer coefficient using an inverse formulation within the FE software to generate the appropriate HTC for this material (Figure 3b).

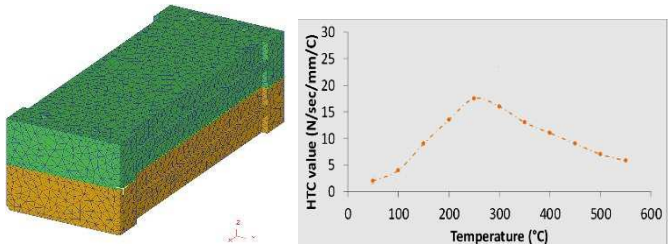

Fig. 3. (a) Inter-object relationship to model the two workpieces joined; (b) Heat transfer coefficient profiles used during the quenching simulation

3.2. Machining distortion model set up

After the heat treatment process; the machining distortion model was set up for the asymmetric residual stress model. The machining distortion simulation was performed by deleting elements on the heat treatment model, at a similar location as the experimental trials. The element deletion was done using an internal BOOLEAN function in the DEFORM software. During material removal simulation, the sample was constrained in all directions by the boundary conditions at the locations shown in Figure 4. During material removal, the residual stress redistributes depending on depth of cut. In order to achieve equilibrium during this redistribution, distortions occurs.

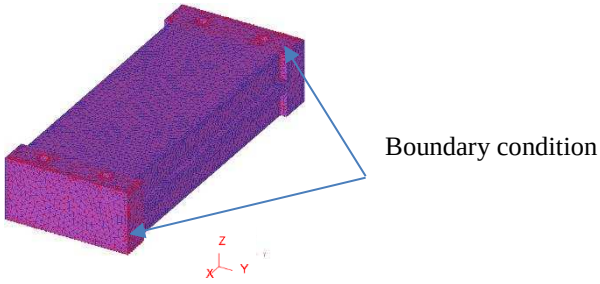

Fig. 4. Boundary constraint applied to machining distortion models.

4. Results and discussions

4.1. Asymmetrical residual stress analysis

The comparison between the FE models and measurements is illustrated in Figures 5 and 6. It can be seen that the FE model predicts the asymmetric residual stresses well for experimental coupons 1 and 2 with around 10 % difference respectively.

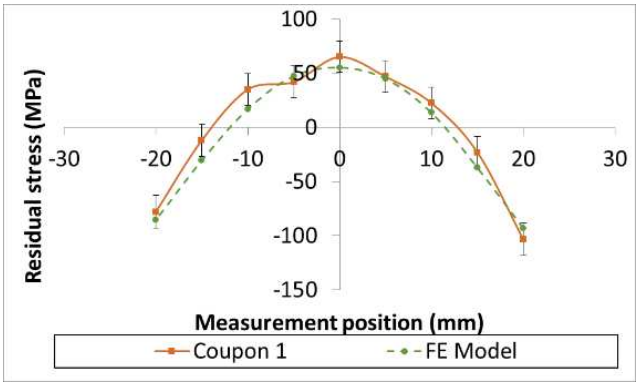

Fig. 5. Asymmetric residual stress measurements from quenching process of coupon 1 compared with FE model.

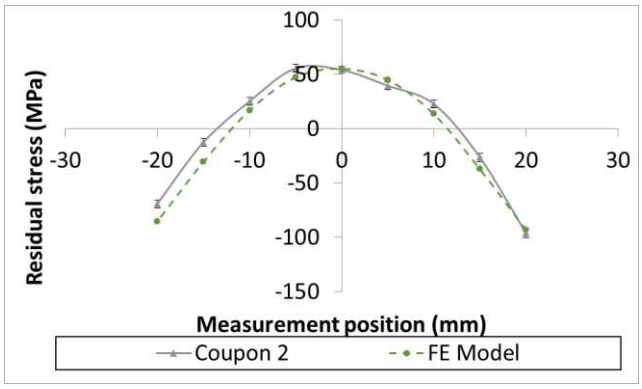

Fig. 6. Asymmetric residual stress measurements from quenching process of coupon 2 compared with FE model.

Experimental residual stress measurements were also taken after the machining of the top face of the coupons, and compared with the FE model. Figure 7 and Figure 8 illustrate that the FE model predicts the trends, but overestimate the residual stress data of coupons 1 and 2 with 22 % (positions -5, 5 to 20 mm) and 28 % (position -5 mm to 0 mm, 10 to 20 mm), respectively. Note that differences of over 100 % were found in the bulk at the centre line location (0 mm) of coupon 1 (Figure 7); and at 5 mm from the centre line for coupon 2 (Figure 8). The figures also show that the stresses have redistributed asymmetrically and have reduced by 70 % after the machining of the top face.

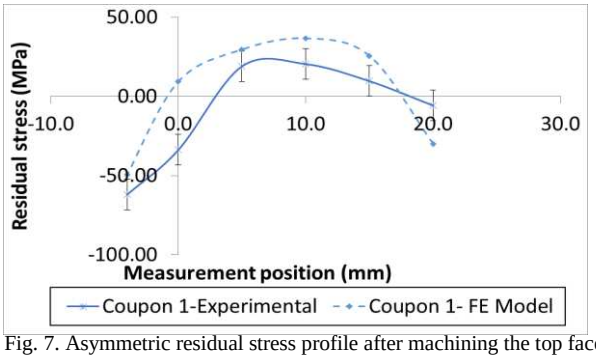

Fig. 7. Asymmetric residual stress profile after machining the top face of coupon 1

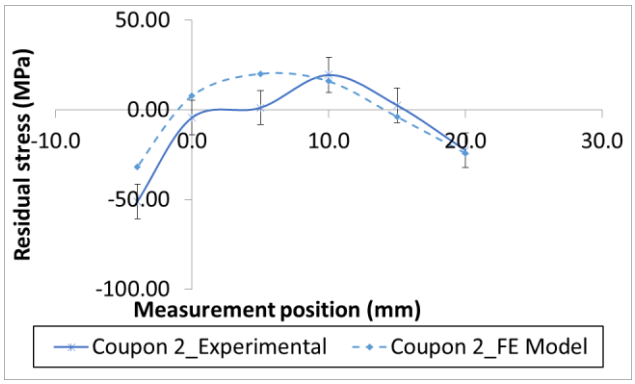

Fig. 8. Asymmetric residual stress profile after machining the top face of coupon 2

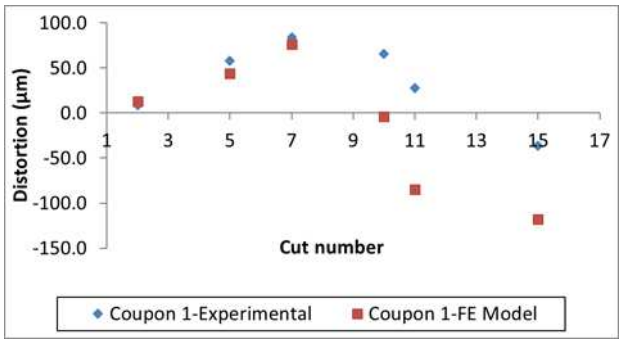

Fig. 9. Machining distortion comparison between FE and experimental data for the asymmetric residual stress of coupon 1

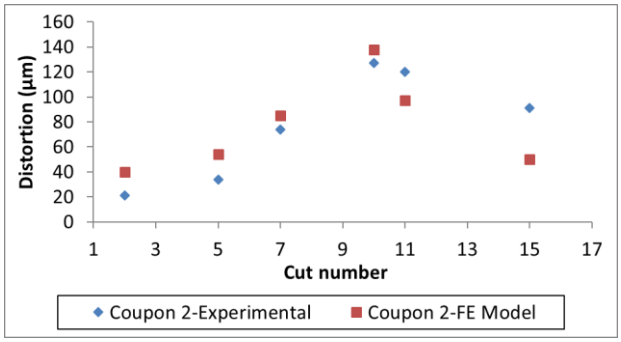

Fig. 10. Machining distortion comparison between FE and experimental data for the asymmetric residual stress of coupon 2

4.2. Machining distortion analysis

After the residual stress analysis of the quenching process, a FE-based virtual machining distortion simulation study was carried out by applying Boolean operations to propose the experimental selection of the machining cuts. In order to propose the different cuts, the virtual simulations were used to investigate comprehensibly the impact of the layer material removal in terms of depths of cut on the redistribution of the residual stress profile into the part, and how this redistribution influences the distortions in the component. Finally, this investigation allowed determining a robust machining approach capable of predicting the final desired distortion magnitudes irrespective of the highly asymmetric residual stress condition of the part.

The FE model accurately predicted the trend in the top face machining distortion for coupon 1 with a difference of 18 %; however, after machining the bottom face of the same coupon the FE model predicted the tendency of the experimental distortion profile, but the magnitude was largely over predicted with a maximum of 42 % difference (Figure 9). This was not the case for coupon 2 with an under predicted difference of 27 % for the top face and an over predicted 38 % difference for the bottom machined face (Figure 10). Similar to the results obtained from the symmetric residual stress profile coupons, the FE model and measurement data were in acceptable agreement for the top face machining. The major differences between the models and distortion data were observed from phase two machining (bottom face machining), which could be due to the model not predicting the stress distribution accurately as previously discussed.

Generally, great distortions occur after fixture release and it is crucial to control those distortions at the point of release regardless of whether an optimized distortion strategy was achieved during machining. The distortion magnitude in turn is influenced by the amount of stresses generated during machining. Figure 11 and 12 illustrate the CMM measurements and the results of the simulations after the fixture release. The measurement points (1-5) were taken at the mid width bottom surface of the coupon. It can be seen from Figure 11 that the distortion prediction for points 1 and 2 have a difference of over 100% and 50% respectively. For Figure 12, the distortion prediction has a maximum error of 100% and 20% for points 1 and 2. Both models under predicted the distortions for points 3 to 4 as shown in Figure 11 and 12.

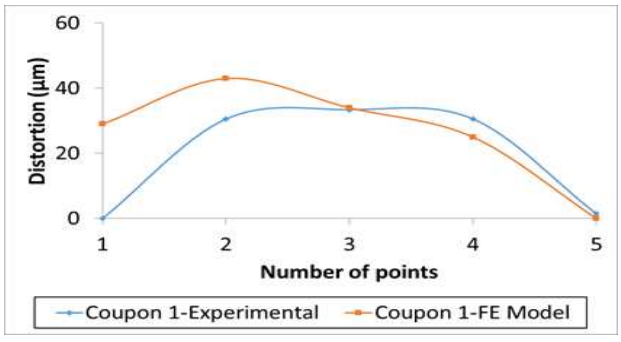

Fig. 11. CMM distortion measurement after fixture release compared to the distortion of the asymmetric residual stress FE model of coupon 1

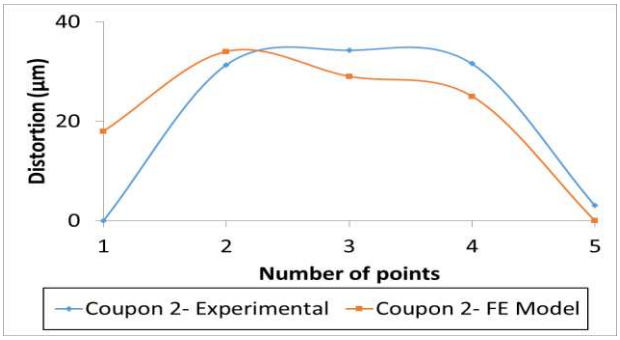

Fig. 12. CMM distortion measurement after fixture release compared to the distortion of the asymmetric residual stress FE model of coupon 2

5. Conclusions

In this paper, a FE-based numerical modelling was developed for predicting the machining distortion in order to achieve a given tolerance with asymmetrical residual stress profile.

Firstly, neutron diffraction was used to capture the generated asymmetrical residual stress profile after the heat treatment process, and the redistributed residual stresses after machining of the top face of the coupons. This allowed to validate the developed FE model for predicting residual stresses and after quenching and machining.

Finally, the machining distortion model was successfully implemented to investigate comprehensibly the impact of the layer material removal in terms of depths of cut on the redistribution of the residual stress profile into the part, and to analyse how this redistribution influences the distortions in the coupon. This investigation has developed a robust machining approach capable of predicting a final desired distortion tolerance magnitude after clamping of 50 µm, irrespective of the highly asymmetric residual stress condition of the coupon.

It should be noted that in most cases the FE model predicted the trends and magnitudes of the both the stresses and distortion of the coupons, although further work needs to be performed for more accurate predictions.

References

[1] Qian Zhang, Mahdi Mahfouf , John R. Yates, Christophe Pinna, George Panoutsos,Soufiene Boumaiza, Richard J. Greene, Luis de Leon. Modeling and Optimal Design of Machining-Induced Residual Stresses in Aluminium Alloys Using a Fast Hierarchical Multiobjective Optimization Algorithm. Psychol. Sci. vol. 28. no. 1. pp. 80–91; 2011.

[2] X. Z. Wang. Research and Optimization on NC Milling Technology for Two Typical Aeronautical Materials. Dalian University of Technology (People's Republic of China); 2005.

[3] X. Huang. Effects of milling process sequence on the residual stress related monolithic components deformation. no. Icmit. pp. 301–306; 2017.

[4] J. Mackerle, C. W. Wu, and B. Liu. A review of inducing compressive residual stress – shot peening; on structural metal and welded connection; 2017.

[5] P. Stress. 1 . Machine Distortion,. vol. 61. no. 1; 1991.

[6] X. Cerutti, K. Mocellin, Influence of the machining sequence on the residual stress redistribution and machining quality: Analysis and improvement using numerical simulations. Int. J. Adv. Manuf. Technol. vol. 83. no. 1–4. pp. 489–503; 2016.

[7] A. Madariaga, P. J. Arrazola, I. Perez, R. Sanchez, J. J. Ruiz, and F. J. Rubio. Reduction of distortion of large aluminium parts by controlling machining-induced residual stresses. pp. 1–15; 2017.

[8] B. Denkena, D. Boehnke, L. León. Machining induced residual stress in structural aluminum parts. Prod. Eng. vol. 2. no. 3. pp. 247–253; 2008.

[9] S. International. Heat Treatment of Aluminum Alloy Raw Materials (AMS2772); 2016.

[10] Renishaw plc. MP700 probe with 360 ° optical transmission system; 2008.

[11] K. Ma et al. Modeling of Residual Stress and Machining Distortion in Aerospace Components. Am. Soc. Met. Handb. vol. 88. ABW–2010. pp. 1–41; 2013.

[12] Knezevic. M, Chun, B.K, Oh. J.Y, Wu. W.-T, Ress III. R.A, Glavicic. M.G, Srivatsa, S. Modeling machining distortion using the finite element method: Application to engine disk. Trans. North Am. Manuf. Res. Inst. SME. vol. 40; 2012.